Int. J. Appl. Comput. Math (2020) 6:16
https://doi.org/10.1007/s40819-019-0765-1

ORIGINAL PAPER

Non-similar Solution of Eyring–Powell Fluid Flow and Heat Transfer with Convective Boundary Condition: Homotopy Analysis Method

Atul Kumar Ray[1] · B. Vasu[1] · P. V. S. N. Murthy[2] · Rama S. R. Gorla[3]

Abstract
The study presents the mixed convective boundary layer flow of Eyring–Powell fluid over a vertical plate with variable velocity and temperature distribution taking convective boundary condition into account. The transformed non-dimensional governing equations in non-similar nature are solved by employing hybrid technique: local non-similarity method in conjunction with homotopy analysis method. The convergence of homotopy series solution is obtained and presented for various order of approximations. The series solutions have been validated by comparing the results available in the literature and found good agreement. The obtained results are shown properly by graphs and discussed for various values of thermo-physical parameters. It is found that the Eyring–Powell fluid shows higher velocity than Newtonian fluid whereas lower temperature than Newtonian fluid. Furthermore as increase in fluid parameter, ratio of relaxation and retardation parameter, skin friction coefficient decreased and heat transfer coefficient increased. The study finds wide applications in the field of design of heat exchangers, process of cooling of metallic plate, extrusion of plastic sheets, in polymer and glass industries etc.

Keywords Eyring–Powell fluid · Mixed convection · Convective boundary condition · Local non-similarity method · Homotopy analysis method

✉ B. Vasu
bvasu@mnnit.ac.in

Atul Kumar Ray
rma0215@mnnit.ac.in

P. V. S. N. Murthy
pvsnm@maths.iitkgp.ernet.in

Rama S. R. Gorla
r.gorla@csuohio.edu

[1] Department of Mathematics, Motilal Nehru National Institute of Technology, Prayagraj 211004, India

[2] Department of Mathematics, Indian Institute of Technology Kharagpur, Kharagpur 721302, India

[3] Department of Mechanical Engineering, Cleveland State University, Cleveland, OH 44115, USA

Published online: 09 January 2020

List of Symbols

A	Cauchy stress tensor (N/m^2)
A_1	Kinematical tensor (N/m^2)
C_f	Local skin friction coefficient
C_p	Specific heat at constant pressure (J/kg K)
c	Fluid parameter (s^{-1})
De	Deborah number
f	Non-dimensional stream function velocity
f_0	Initial guess for non-dimensional velocity
g	Gravitational acceleration (m/s^2)
Gr	Grashof number
n	Power index
Nu	Local Nusselt number
P	Pressure (Pa or N/m^2)
p	Embedded parameter
I	Identity vector
Pr	Prandtl number
Re	Reynolds number
T	Fluid temperature (K)
V	Velocity vector (m/s)
u, v	Dimensional velocity components (m/s)
x, y	Cartesian coordinates

Greek Symbols

α	Thermal diffusivity (m^2/s)
β	Fluid parameter
γ	Biot number
$\dot{\gamma}$	Shear rate (s^{-1})
τ	Extra stress tensor (Pa or N/m^2)
τ_w	Shear stress (Pa or N/m^2)
q_w	Rate of heat transfer (W/m^2)
μ	Dynamitic viscosity (Pa s)
υ	Kinematic viscosity of the fluid (m^2/s)
θ	Dimensionless temperature
ψ	Stream function (m^2/s)
ξ	Mixed convection parameter
η	Non-similarity variables
ρ	Density of fluid (kg/m^3)
$\hbar_i$	Control parameter for f, g and h
$\mathcal{L}_i$	Auxiliary linear operator
$\mathcal{N}_i$	Auxiliary non-linear operator

Subscripts

w	Wall condition
∞	Ambient condition

Superscripts

$'$	Prime denotes the derivative with respect to η

Introduction

The flow and heat transfer [1] due to the continuous stretching plate are important because of their large number of applications in engineering such as the design of heat exchangers, strand casting, the liquid film condensation process, wire drawing, extrusion of plastic sheets and in the polymer and glass industries etc. Sakiadis [2] has studied and formed the solution numerically for the flow of a stretching surface. The problem of Sakiadis has been continued by Erickson et al. [3] with effect of suction/blowing at the moving surface for heat and mass transfer with in boundary layer regime. Karwe and Jaluria [4] have explained the importance of mixed convection flow over continuous moving plate for manufacturing process. Vajravelu and Roper [5] explained the influence of heat generation/absorption and viscous dissipation along with non-linear surface temperature on the flow of non-Newtonian fluid over stretching surface. Magyari et al. [6] have used the self-similar method to yield the solutions for the continuous surface stretched with decelerating velocities. Further, Patilet al. [7] investigated the unsteady mixed convection flows along power law stretching sheet with variable temperature distribution. Mustafa et al. [8] analyzes the influence of free convection on flow of a non-Newtonian fluid past a continuously stretching surface. The flow and heat transfer for a nanofluid over an unsteady stretching plate is studied extensively by Ahmadi et al. [9]. Rao et al. [10] have described the influence of slip condition on the flow of a Casson fluid flow over stretching surface.

The dynamical study of non-Newtonian fluids yields challenge to researchers and scientists. Many industrial fluid (gas–liquid dispersions, coal in water, sewage sludge, foams), biological fluids (blood, salvia, synovial fluid), foodstuffs (soups, jams, jellies), synthetic lubricants, such as cosmetics, toiletries, paints and their flow behaviours are non-linear in nature. The constitutive relations for such fluids lead to higher order and highly complex equations. So, different models of non-Newtonian fluid [11–13] have been developed to deal with such complexity. One of such complex non-Newtonian fluid model is Eyring–Powell fluid model which is capable to describe relaxation theory of viscosity. The Eyring–Powell model [14] has some advantages over the other non-Newtonian fluid models. Instead of empirical relation, the Eyring–Powell fluid model is deduced from kinetic theory of liquid. As per kinetic theory of liquid, bond of the liquid molecules can be either weak or strong. Weaker molecular bond corresponds to the Newtonian relation and strong molecular bond corresponds to the non-Newtonian relation in Eyring–Powell fluid model. So, Eyring–Powell fluid has ability to give Newtonian plateau at low and/or high shear rate, that is, it can overcome the difficulties of power law fluid [15] and Spriggs fluid model [16]. The impact of convective boundary surface on the flow of Eyring–Powell fluid is examined by Hayat et al. [17]. Unsteady flow of Eyring–Powell fluid in presence of magnetic field and thermal radiation is analysed by Ghadikolaei et al. [18]. The influence of homogeneous-heterogeneous reaction on the flow of Eyring–Powell fluid over rotating disc is investigated by Gholinia et al. [19].

Now a day, studies on boundary layer problem with convective boundary condition have attracted researchers due to its importance in technological and industrial fields to adjust thermal effects industrial outputs such as in computer power supply, electronic devices and engine cooling system. The concept of convective boundary condition was initiated by Aziz [20]. Bataller [21] has extended this problem with thermal radiation by considering the Blasius and Sakiadis flows. Khan and Gorla [22] investigated the impact of convective boundary on the flow of non-Newtonian nanofluids over a sheet. Murthy et al. [23] analysed the natural convection flow from a vertical non-Darcy porous plate with convective boundary condition. Ram

Reddy et al. [24] discussed the Soret effect on mixed convection flow of nanofluid past a vertical plate with convective boundary conditions. Kameswaran et al. [25] investigated the influence of convective boundary condition and radiation on the flow of nanofluid past a permeable flat plate. Vasu et al. [26] have provided the analysis of nonlinear temperature density and entropy generation in Newtonian fluid flow over a porous plate with convective surface.

The non-similarity flow problems are more general in real life, and hence retain wider importance than the similarity flows. The local similarity method [27] is used to deal with non-similar boundary layer flow problems. But the local-similarity method has some limitations that the results found are of unreliable verity due to the removal of streamwise derivatives and there is no positive way to validate the impact of these removals on the final results. The method of local non-similarity was unfolded by Sparrow and Yu [28]. Rao et al. [8] analysed the effect of mixed convection heat transfer on boundary layer flow of Casson fluid past a stretching surface by employing non-similar transformation. Mushtaq et al. [29] employed different methodologies namely, finite difference, perturbation and local non-similarity method to explore the influence of mixed convection flow of non-Newtonian fluid past a continuous stretching surface. Vasu and Ray [30] have provided the local non-similar solution in conjunction with the homotopy analysis method to the flow of Carrareu nanofluid over a plate with Cattaneo–Christov heat flux model.

It may be noticed that past survey did not receive the influence of convective boundary condition on non-similar solution of mixed convection flow of Eyring–Powell fluid past a vertical plate. Here the free fall of a flat (vertical) plate inside an Eyring–Powell fluid is considered. Hence, the scope of the current article is to obtain local non-similar solution to the mixed convection flow of Eyring–Powell fluid over vertical plate with condition of convective boundary and variable surface temperature. Further, present study shows the computational aspects of first and second level of truncation of non-similarity methods. An analytical method namely the homotopy analysis method (HAM) [31–34], is applied nicely to obtain the series solution of the problem. Variation of velocity and temperature for different Prandtl number, mixed convection parameter and fluid parameter is shown graphically. Coefficient of skin friction is reduced with rise in Prandtl number and Local Nusselt number is increased with Prandtl number.

Mathematical Formulation

We considered steady two-dimensional mixed convection flow of Eyring–Powell fluid along a vertical stretched flat plate with convective boundary condition. It is assumed that the body force is absent in momentum equation and viscous dissipation is neglected in the energy equation. Here x-axis is parallel to the plate while y-axis is perpendicular to x-axis. u and v are the velocity component in the direction of x and y respectively. The schematic diagram of the problem is shown in Fig. 1 and includes full details of model and assumption.

For Eyring–Powell fluid [17], the Cauchy stress tensor can be written as

$$A = -PI + \tau \tag{1}$$

whereas pressure P and identity I appears in (1). τ is extra stress tensor and is given by

$$\tau = \left(\mu + \frac{1}{\delta\dot{\gamma}} \sinh^{-1}\left(\frac{1}{c}\dot{\gamma}\right)\right) A_1 \tag{2}$$

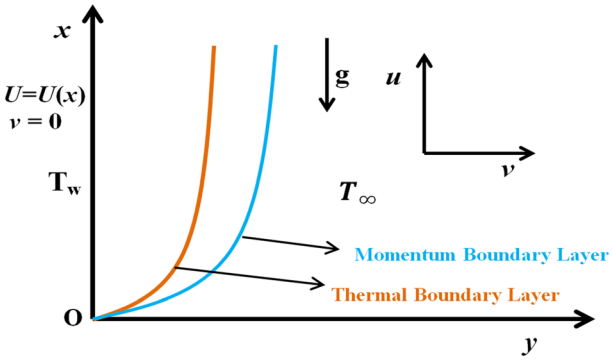

Fig. 1 Schematic Diagram of the problem

where δ and c are the parameters of fluid, μ is the dynamic viscosity and c having $(\text{time})^{-1}$ dimension. $\sinh^{-1}\left(\frac{1}{c}\dot{\gamma}\right)$ is expressed as

$$\sinh^{-1}\left(\frac{1}{c}\dot{\gamma}\right) \cong \frac{1}{c}\dot{\gamma} - \frac{1}{6}\left(\frac{1}{c}\dot{\gamma}\right)^3 \quad \text{with} \left(\frac{\dot{\gamma}}{c}\right)^5 <<< 1$$

Therefore from (2),

$$\tau = \left(\mu + \frac{1}{\delta c}\right)A_1 - \frac{1}{6\delta c^3}(\dot{\gamma})^2 A_1 \tag{3}$$

Here value of $\dot{\gamma} = \sqrt{\frac{1}{2}trA_1^2}$ and A_1 is kinematical tensor and given as $A_1 = \nabla V + (\nabla V)^T$, with V as velocity vector.

Under the assumption of flow condition and using boundary layer approximation, conservation equations that govern the flow [29] are:

$$\frac{\partial u}{\partial x} + \frac{\partial v}{\partial y} = 0 \tag{4}$$

$$u\frac{\partial u}{\partial x} + v\frac{\partial u}{\partial y} = \left(\upsilon + \frac{1}{\rho c\delta}\right)\frac{\partial^2 u}{\partial y^2} - \frac{1}{2\rho\delta c^3}\left(\frac{\partial u}{\partial y}\right)^2\frac{\partial^2 u}{\partial y^2} + g\beta(T - T_\infty) \tag{5}$$

$$u\frac{\partial T}{\partial x} + v\frac{\partial T}{\partial y} = \alpha\frac{\partial^2 T}{\partial y^2} \tag{6}$$

And conditions at boundary are

$$\text{At } y = 0, \quad u = U(x), \quad v = 0, \quad -k\frac{\partial T}{\partial y} = h(T_w - T) \tag{7}$$

$$y \to \infty, \quad u = 0, \quad T = T_\infty \tag{8}$$

The flow is caused by continuous stretching of plate and the buoyancy effect. Also, the plate is under convective boundary condition (Eq. (7)) and free stream velocity is zero (Eq. (8)). Equations (4)–(8) will undergo the non-similar transformation for getting non-similar solution. Non-similarity transformation converts the physical coordinates x,

y into the new coordinates η, ξ. η is known as pseudo-similarity variables and contains both physical coordinates x and y where ξ is function of x only. Let ψ is stream function and non-similarity and dimensionless variables as,

$$\psi = \nu \mathrm{Re}^{1/2} f(\eta, \xi), \quad \eta = \frac{y}{x}\mathrm{Re}^{1/2}, \quad \xi = \frac{\mathrm{Gr}_x}{\mathrm{Re}_x^2} \tag{9}$$

where $\mathrm{Re}_x = \frac{Ux}{\nu}$ and $\mathrm{Gr}_x = \frac{g\beta\Delta T x^3}{\nu^2}$ are Reynolds number and Grashof number respectively. Forced convection dominates the flow field for small value of mixed convection parameter ξ and buoyancy forces dominate the flow field for large value of ξ.

ψ is stream function for which $u = \frac{\partial \psi}{\partial y}, v = -\frac{\partial \psi}{\partial x}$. Continuity equation is satisfied automatically. Here we considered the following form of velocity and temperature of the surface:

$$U(x) = U_0 x \quad \text{and} \quad \Delta T(x) = T_0 x^2$$

The transformed boundary layer non-dimensional momentum and energy equations are

$$(1+\varepsilon) f''' + f f'' - \left(f'\right)^2 - \varepsilon \delta f''' \left(f''\right)^2 + \xi\theta = \xi\left(f' \frac{\partial f'}{\partial \xi} - f'' \frac{\partial f}{\partial \xi}\right) \tag{10}$$

$$\frac{1}{\mathrm{Pr}}\theta'' + f\theta' - 2\theta f' = \xi\left(f' \frac{\partial \theta}{\partial \xi} - \theta' \frac{\partial f}{\partial \xi}\right) \tag{11}$$

conditions at boundary becomes,

$$\begin{aligned} &f(0,\xi) = 0, \quad f'(0,\xi) = 1, \quad \theta'(0,\xi) = -\gamma(1 - \theta(0,\xi)) \\ &f'(\infty,\xi) = 0, \quad \theta(\infty,\xi) = 0 \end{aligned} \tag{12}$$

where

$$\varepsilon = \frac{1}{\rho \delta c \upsilon}, \quad \mathrm{Pr} = \frac{\upsilon}{\alpha}, \quad \gamma = \frac{hx}{k(\mathrm{Re})^{1/2}}, \quad \text{and} \quad \lambda = \frac{\upsilon^2 (\mathrm{Re})^3}{2c^2 x^4}$$

γ is Biot number and material fluid parameters are represented by ε and λ, prime appears in the Eqs. (10)–(12) denotes derivative with respect to η, Pr is Prandtl number. The local skin friction coefficient c_f and Nusselt number Nu are also calculated by using following equations for practical applications

$$c_f = \mu \frac{2\tau_w(x)}{\rho (U(x))^2} \tag{13}$$

and

$$\mathrm{Nu} = \frac{q_w(x) x}{k \Delta T} \tag{14}$$

where

$$\tau_w = \left[\mu\frac{\partial u}{\partial y} + \frac{1}{\delta c}\frac{\partial u}{\partial y} - \frac{1}{6\delta c^3}\left(\frac{\partial u}{\partial y}\right)^3\right]_{y=0}$$

And

$$q_w = -k\left(\frac{\partial T}{\partial y}\right)_{y=0} \tag{15}$$

Furthermore, after introducing transformation Eq. (9) in Eq. (15), from Eq. (13), the dimensionless skin friction become

$$\frac{1}{2}\mathrm{Re}^{1/2}c_f = (1+\varepsilon)f''(0,\xi) - \frac{\lambda\varepsilon}{3}\left(f''(0,\xi)\right)^3 \tag{16}$$

Similarly, the local Nusselt number from Eq. (14) can be expressed as

$$\mathrm{Re}^{-1/2}\mathrm{Nu} = -\theta'(0,\xi) \tag{17}$$

Non-similarity Method

Similarity and non-similarity schemes are basically two different methods for finding the solution in boundary layer problems. The solution process of similarity method is easier. But in many physical problems, similarity solution do not exists. Like, the free and mixed convection flow over vertical plate is in general non-similar. So, when such problems do not pursue the similarity solution. One had to solve such problems using non-similarity method. The non-similarity method has been use to solve complex problems by many researchers [35–39]. These methods are given in the text book of Minkowycz et al. [40].

First Level of Truncation (Local Similarity)

Local similarity method [27] is one of the frequently used non-similar methods. This method is computationally simple and admits non-similar solution to boundary layer problems. An interesting aspect of this method is that once the governing equations transformed, then those equations can be treated as ordinary differential equation by considering the non-similarity terms as small enough so that these term can be taken as zero. Also by means of local similarity method, solution at any particular streamwise location can be obtained without any further calculations at upstream location. The method of local similarity has been implemented by many researches [41–43] For local similarity solution, the right hand side terms of Eqs. (10) and (11) containing $\xi.\frac{\partial(.)}{\partial\xi}$ are approximated as very smalland hence are deleted from Eqs. (10) and (11) which is possible when $\xi \ll 1$. So the local similarity leads us to the following system of equations:

$$(1+\varepsilon)f''' + ff'' - \left(f'\right)^2 - \varepsilon\lambda f'''\left(f''\right)^2 + \xi\theta = 0 \tag{18}$$

$$\frac{1}{\mathrm{Pr}}\theta'' + f\theta' - 2\theta f' = 0 \tag{19}$$

$$f(0,\xi)=0,\quad f'(0,\xi)=1,\quad \theta'(0,\xi)=-\gamma(1-\theta(0,\xi)),\quad f'(\infty,\xi)=0,\quad \theta(\infty,\xi)=0 \tag{20}$$

It can be seen that equations Eqs. (18)–(20) are system of ordinary differential equations for f and θ where ξ treat as parameter.

Local Non-similarity Method

The solutions obtained by local-similarity method are of uncertain accuracy which is its major limitation. It is obvious that the final result will be affect due to the removal of streamwise derivatives. Thus these non-similarity terms must be considered to improve the verity of the solution. Sparrow et al. [28, 44, 45] introduced the method of local non-similarity method. Massoudi [45] applied local non-similarity method to flows of non-Newtonian fluid over a wedge. Mureithi and Mason [46] analysed the mixed convection flow over the plate with variable free-stream velocity and temperature at the wall. The effect of viscous dissipation is also taken into account.

The non-similarity bearing of the Eqs. (10)–(12) are demonstrated in the terms containing $\frac{\partial f}{\partial \xi}$ and $\frac{\partial \theta}{\partial \xi}$, So, to find the second level of truncation and to eliminate the presence of the terms $\frac{\partial f}{\partial \xi}$ and $\frac{\partial \theta}{\partial \xi}$, we introduce the following functions:

$$g(\eta,\xi)=\frac{\partial f}{\partial \xi},\ \phi(\eta,\xi)=\frac{\partial \theta}{\partial \xi}$$

Equations (10)–(12) reduces to:

$$(1+\varepsilon)f'''+ff''-\left(f'\right)^2-\lambda\varepsilon f'''\left(f''\right)^2+\xi\theta=\xi\left(f'g'-f''g\right) \tag{21}$$

$$\frac{1}{\mathrm{Pr}}\theta''+f\theta'-2\theta f'=\xi\left(f'\phi-\theta' g\right) \tag{22}$$

$$f(0,\xi)=0,\quad f'(0,\xi)=1,\quad \theta'(0,\xi)=-\gamma(1-\theta(0,\xi)),\quad f'(\infty,\xi)=0,\quad \theta(\infty,\xi)=0 \tag{23}$$

Supplementary equations for g and ϕ its boundary conditions can be obtain by differentiating equations Eqs. (21)–(23) w.r.t η. This yield

$$(1+\varepsilon)g'''+fg'+2f''g-3f'g'-\lambda\varepsilon(g'''\left(f''\right)^2+2f'''f''g'')+\theta+\xi\phi=\xi\left(\left(g'\right)^2-g''g\right) \tag{24}$$

$$\frac{1}{\mathrm{Pr}}\phi''+2g\phi'+f\phi'-3\phi f'-2\theta g'=\xi\left(g'\phi-\phi' g\right) \tag{25}$$

$$g(0,\xi)=0,\quad g'(0,\xi)=0,\quad \phi'(0,\xi)=\gamma\phi(0,\xi),\quad g'(\infty,\xi)=0,\quad \phi(\infty,\xi)=0 \tag{26}$$

At second level, the terms containing derivative of g and ϕ with respect to ξ and their higher order terms are deleted. The non-similar solution of system of ordinary differential equations Eqs. (21) and (22) and Eqs. (24) and (25), along with boundary conditions Eqs. (23) and (26) are solved via HAM.

Solution by HAM

Analytic solutions to the governing equation obtain from classical hydrodynamics problems like boundary layers flow over a flat plate are difficult to obtain. There are several attempts have been used to solve such governing equations using analytic methods. Applications of analytic methods like variational iteration and homotopy-perturbation method is elaborated by Ganji et al. [47] for solving non-linear heat diffusion and heat transfer equations. These methods depend on small/large physical parameters which raise difficulties in solving the complex hydrodynamic problems. The homotopy analysis method (HAM) developed by Liao [30, 48] is a semi analytic method which does not depend on any parameter since it is based on the homotopy, a topological concept. The HAM is admirably used to solve many non-linear problems based on real life problems such as the non-homogeneous Blasius problem [49], the nano boundary layer flows [50], MHD Newtonian flow in a semi-porous channel [51] and the flows over a porous wedge [52]. Recently, Hassan and Rashidi [53] employed HAM to show effect of Reynolds number on micropolar flow in porous channel by considering the mass injection into account. Dinarvand et al. [54] used HAM to investigate the heat transfer flow of water based nanofluid past a circular cylinder. Vasu et al. [55] implemented HAM to solve a partial differential equation arising from the flow of Spriggs fluid past oscillatory moving plate. Ray et al. [56] studied electrically-conducting Casson nanofluid bioconvection thin film transport phenomena from a time-dependent stretching sheet using HAM. These applications explain the fine ability of HAM for solving strong non-linear problems. In previous section, the analytic solution for velocity and temperature field has been obtained. They found that the copper–water nanofluid enhance more heat transfer rate when compared with titania-water nanofluid and alumina-water nanofluid.

In this section, system of equations Eqs. (21)–(23) together with auxiliary system of equations Eqs. (24)–(26) are solved by employing HAM with appropriate initial guess f_0 and θ_0 are given as:

$$f_0 = 1 - e^{-\eta} \tag{27}$$

$$\theta_0 = \frac{\gamma}{\gamma + 1} e^{-\eta} \tag{28}$$

And linear operators are chosen as

$$\mathcal{L}_1(f) = f''' - f', \quad \mathcal{L}_2(\theta) = \theta'' - \theta \tag{29}$$

satisfying the properties

$$\mathcal{L}_1(A_1 + A_2 e^{\eta} + A_3 e^{-\eta}) = 0, \quad \mathcal{L}_2(B_1 e^{\eta} + B_2 e^{-\eta}) = 0 \tag{30}$$

Here, A_m's ($m = 1$ to 3) and B_k's ($k = 1, 2$) are arbitrary constants. Considering known parameter $p \in [0, 1]$ as embedding parameter, h_1 and h_2, as non-zero convergence control parameters, then we can construct the zeroth-order deformation equations as

$$(1 - p)\mathcal{L}_1[f(\eta, \xi; p) - f_0(\eta, \xi)] = p h_1 \mathcal{N}_1[(f(\eta, \xi; p), \theta(\eta, \xi; p))] \tag{31}$$

$$(1 - p)\mathcal{L}_2[\theta(\eta, \xi; p) - \theta_0(\eta, \xi)] = p h_2 \mathcal{N}_2[(f(\eta, \xi; p), \theta(\eta, \xi; p))] \tag{32}$$

subject to following boundary conditions

$$\begin{aligned} f(0,\xi;p) = 0, \quad f'(0,\xi;p) = 1, \quad \text{and} f'(\infty,\xi;p) = 0 \\ \theta'(0,\xi;p) = -\gamma(1-\theta(0,\xi;p)), \quad \theta(\infty,\xi;p) = 0 \end{aligned} \tag{33}$$

The nonlinear operators is chosen as

$$\begin{aligned} \mathcal{N}_1(f(\eta,\xi;p),\theta(\eta,\xi;p)) = (1+\varepsilon)\frac{\partial^3 f(\eta,\xi;p)}{\partial\eta^3} + f(\eta;p)\frac{\partial^2 f(\eta,\xi;p)}{\partial\eta^2} - \left(\frac{\partial f(\eta,\xi;p)}{\partial\eta}\right)^2 \\ - \lambda\varepsilon\frac{\partial^3 f(\eta,\xi;p)}{\partial\eta^3}\left(\frac{\partial^2 f(\eta,\xi;p)}{\partial\eta^2}\right)^2 \\ - \xi\left(\frac{\partial f(\eta,\xi;p)}{\partial\eta}\frac{\partial f'(\eta,\xi;p)}{\partial\xi} - \frac{\partial f^2(\eta,\xi;p)}{\partial\eta^2}\frac{\partial f(\eta,\xi;p)}{\partial\xi}\right) \end{aligned} \tag{34}$$

$$\begin{aligned} \mathcal{N}_2(f(\eta,\xi;p),\theta(\eta,\xi;p)) = \frac{1}{\mathrm{Pr}}\frac{\partial^2\theta(\eta;p)}{\partial\eta^2} + f(\eta,\xi;p)\frac{\partial\theta(\eta,\xi;p)}{\partial\eta} - 2\theta(\eta,\xi;p)\frac{\partial f(\eta,\xi;p)}{\partial\eta} \\ - \xi\left(\frac{\partial f(\eta,\xi;p)}{\partial\eta}\frac{\partial\theta(\eta,\xi;p)}{\partial\xi} - \frac{\partial\theta(\eta,\xi;p)}{\partial\eta}\frac{\partial f(\eta,\xi;p)}{\partial\xi}\right) \end{aligned} \tag{35}$$

For $p = 0$, we have

$$f(\eta,\xi;0) = f_0(\eta,\xi), \quad \theta(\eta,\xi;0) = \theta_0(\eta,\xi) \tag{36}$$

and for $p = 1$, we get

$$f(\eta,\xi;1) = f(\eta,\xi), \quad \theta(\eta,\xi;1) = \theta(\eta,\xi) \tag{37}$$

thus, as p changes from 0 to 1, value of $f(\eta,\xi;p)$ deforms $f_0(\eta,\xi)$ $f(\eta,\xi)$ and similarly $\theta(\eta,\xi;p)$ deforms from $\theta_0(\eta,\xi)$ to $\theta(\eta,\xi)$.

Further, $f(\eta,\xi;p)$ and $\theta(\eta,\xi;p)$ are expanded using Taylor's series with respect to p,

$$f(\eta,\xi;p) = f_0(\eta,\xi) + \sum_{r=1}^{\infty} f_r(\eta,\xi)p^r \tag{38}$$

$$\theta(\eta,\xi;p) = \theta_0(\eta,\xi) + \sum_{r=1}^{\infty} \theta_r(\eta,\xi)p^r \tag{39}$$

where

$$\begin{aligned} f_r(\eta,\xi) = \frac{1}{r!}\frac{\partial^r f(\eta,\xi;p)}{\partial p^r}|_{p=0} \\ \theta_r(\eta,\xi) = \frac{1}{r!}\frac{\partial^r \theta(\eta,\xi;p)}{\partial p^r}|_{p=0} \end{aligned} \tag{40}$$

By setting suitable initial guess, auxiliary linear operators and convergence control parameters the series Eqs. (38) and (39) are converges at $p = 1$, hence the series solution are obtained as follows:

$$f(\eta,\xi) = f_0(\eta,\xi) + \sum_{r=1}^{\infty} f_r(\eta,\xi) \tag{41}$$

$$\theta(\eta,\xi) = \theta_0(\eta,\xi) + \sum_{r=1}^{\infty} \theta_r(\eta,\xi) \tag{42}$$

Now, r^{th}-order deformation equations can be found by differentiating Eqs. (31)–(33) r times with respect to p, taking $p = 0$ and then divide by $r!$, thus Eqs. (31)–(33) changes to

$$\mathcal{L}_1[f_r(\eta,\xi) - \chi_r^* f_{r-1}(\eta,\xi)] = h_1 R_r^f(\eta,\xi) \tag{43}$$

$$\mathcal{L}_2[\theta_r(\eta,\xi) - \chi_r^* \theta_{r-1}(\eta,\xi)] = h_2 R_r^\theta(\eta,\xi) \tag{44}$$

with boundary conditions as

$$\begin{aligned} &f_r(0,\xi) = 0, \quad f_r'(0,\xi) = 0 \quad \text{and} \quad f_r'(\infty,\xi) = 0 \\ &\theta_r'(0,\xi) = \gamma\theta_r(0,\xi), \quad \theta_r(\infty,\xi) = 0 \end{aligned} \tag{45}$$

Here,

$$\begin{aligned} R_r^f(\eta,\xi) = {} & (1+\varepsilon) f_{r-1}'''(\eta) + \sum_{i=0}^{r-1} f_{r-1-i}(\eta,\xi) f_i''(\eta,\xi) - \sum_{i=0}^{r-1} f_{r-1-i}'(\eta,\xi) f_i'(\eta,\xi) \\ & - \lambda\varepsilon \sum_{i=0}^{r-1} f_{r-1-i}'''(\eta,\xi) \sum_{j=0}^{i} f_{i-j}''(\eta,\xi) f_j''(\eta,\xi) + \xi\theta_{r-1}(\eta,\xi) \\ & - \xi\left(\sum_{i=0}^{r-1} f_{r-1-i}'(\eta,\xi) \frac{\partial f_i'(\eta,\xi)}{\partial\xi} - \sum_{i=0}^{r-1} f_{r-1-i}''(\eta,\xi) \frac{\partial f_i(\eta,\xi)}{\partial\xi} \right) \end{aligned} \tag{46}$$

$$\begin{aligned} R_r^\theta(\eta,\xi) = {} & \frac{1}{\mathrm{Pr}} \theta_{r-1}''(\eta,\xi) - 2\sum_{i=0}^{r-1} \theta_{r-1-i}(\eta,\xi) f_i'(\eta,\xi) + \sum_{i=0}^{r-1} f_{r-1-i}(\eta,\xi) \theta_i'(\eta,\xi) \\ & - \xi \sum_{i=0}^{r-1} \left(f_{r-1-i}'(\eta,\xi) \frac{\partial\theta_i(\eta,\xi)}{\partial\xi} - \theta_{r-1-i}'(\eta,\xi) \frac{\partial f_i(\eta,\xi)}{\partial\xi} \right) \end{aligned} \tag{47}$$

and

$$\chi_r^* = \begin{cases} 0, & r \le 1 \\ 1, & r > 1 \end{cases} \tag{48}$$

If $f *_r (\eta,\xi)$ and $\theta *_r (\eta,\xi)$ are special solutions of (43) and (44) satisfying boundary condition (44).

Then

$$f_r(\eta,\xi) = f *_r (\eta,\xi) + A_1 + A_2 e^{\eta} + A_3 e^{-\eta} \tag{49}$$

$$\theta_r(\eta,\xi) = \theta *_r (\eta,\xi) + B_1 e^{\eta} + B_2 e^{-\eta} \tag{50}$$

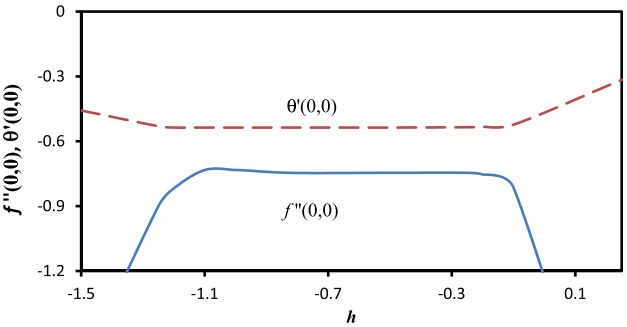

Fig. 2 h-curve

Table 1 Convergence of series solutions for $\Pr = 0.71$, $\varepsilon = \lambda = 1, \gamma = 1, \xi = 0.5$, $h_1 = h_2 = -0.6$

m (order of approximation)	$-f''(0,0)$	$-\theta'(0,0)$
5	−0.75708	−0.535309
10	−0.76174	−0.53572
15	−0.76148	−0.53569
20	−0.76147	−0.53569
25	−0.76147	−0.53569
30	−0.76147	−0.53569

where the values of constants $A_i (i = 1, 2, 3)$ and B_j $(j = 1, 2)$ can be gained by using r$^{\text{th}}$ order deformation boundary condition in (49) and (50). These values are

$$A_1 = -(f *_r (0,\xi) + f *'_r (0,\xi)), \quad A_2 = 0, \quad A_3 = f *'_r (0,\xi)$$
$$B_1 = 0, \quad B_2 = \frac{\theta' *_r (0,\xi) - \gamma\theta *_r (0,\xi)}{1+\gamma}$$

Thus, the series solution (41) and (42) is obtained after substituting (49) in (41) and (50) in (42) respectively.

Convergence of HAM

The series solution of Eqs. (10) and (11) with boundary conditions in Eq. (12) depends on the convergence control parameter h_1 and h_2 which are responsible for controlling the convergence of homotopy series solution as described by Liao [24]. Hence the range of these parameters obtained and depicts h-curve (Fig. 2). It is noted that the range of h_1 and h_2, are $-0.2 < h_1 < 0.8$ and $-0.2 < h_2 < 1.25$. Table 1 presents the convergence of homotopy solution for various order of approximation and it is found that 15$^{\text{th}}$ order of approximation is adequate to consider for computation.

Table 2 Comparison of result with Hayat et al. [57] of approximations for $\Pr = 0.71$, $\varepsilon = 1$, $\lambda = 0.2, \xi = 0$

m (order of approx.)	Hayat et al. [57]		Present result	
	$-f''(0,0)$	$-\theta'(0,0)$	$-f''(0,0)$	$-\theta'(0,0)$
5	0.214032	0.455456	0.2140317	0.453651
10	0.213592	0.454047	0.2135997	0.454063
15	0.213579	0.454109	0.213580	0.454126
20	0.213579	0.454123	0.213578	0.454126
25	0.213579	0.454127	0.213578	0.454126
30	0.213579	0.454127	0.213578	0.454126

Table 3 Comparison of present study with Nataraja et al. [58] and Mushtaq et al. [29] for different values of Prandtl number Pr by considering $\xi = 0, \varepsilon = 0$

Pr	$\theta'(0)$		
	Nataraja et al. [58]	Mushtaq et al. [29]	Present
1	1.3333	1.3349	1.33333
5	3.3165	3.2927	3.31651
10	4.7969	4.7742	4.78967

Result and Analysis

The governing Eqs. (4)-(6) with boundary conditions (7) and (8) are transformed to non-dimensionalised form (10) and (11) with boundary conditions in (12) by using the non-similarity transformation (9). The resultant non-dimensional partial differential Eqs. (10) and (11) with boundary condition (12) are solved by employing non-similarity method in conjunction with HAM. Firstly, partial differential equations are transformed to ordinary differential Eqs. (18) and (19) with boundary condition (20) using first level of truncation (local similarity method) and then approximated second level of truncation shown in (21), (22), (24) and (25) with respect to boundary conditions (23) and (26). Series solution of these systems of differential equations is given by HAM. The obtained results of the present problem for a particular case is compared with study of Hayat et al. [57] shown in Table 2 when $\Pr = 0.71$, $\varepsilon = 1$, $\lambda = 0.2$, $\xi = 0$. The present results are also compared with Mushtaq et al. [29] and Nataraja et al. [58] for different values of Prandtl number Pr in Table 3 when $\xi = 0, \varepsilon = 0$. From Tables 2 and 3, the comparison states that the current results are in excellent agreement.

Following fixed value of parameters are taken for computation:

$\xi = 0.5, \Pr = 0.71$, $\gamma = 1$, $\varepsilon = 0.6$, $\lambda = 1$, $h_1 = h_2 = -0.6$ for similarity solution (first level of truncation)
$\xi = 0.5$, $\Pr = 0.71$, $\gamma = 1$, $\varepsilon = 0.6$, $\lambda = 1$, $h_1 = h_2 = -0.75$ for second level of truncation.

Figure 3 compares the velocity profile obtained in first (local similarity) and second level (local non-similarity) of truncation for different Eyring–Powell fluid parameter ε. Momentum boundary layer thickness is less in local non-similarity method as compare local similarity method. Velocity decays faster to zero for second level of truncation than first level of truncation and this behaviour is due to removal of streamwise differentials

in first level of truncation. Noted that $\xi = 0.5$ is taken in both local similar and local non-similarity method only to compare the variations of velocity and temperature. Figure 4 compares the temperature profile obtained in first and second level of truncation for different Eyring–Powell fluid parameter ε. By using local non-similarity method, the thermal boundary layer thickness is decreased when compared to local similarity method. Further, it is also observed from the Figs. 3 and 4 that the velocity profile falls with increase in ε. Because increasing value of ε leads to decrease in viscosity which results in increase in velocity profile (Fig. 3). The impact of ε on temperature profile displays in Fig. 4 concludes that temperature decreases with ε.

Figures 5 and 6 illustrate the influence of Pr on velocity and temperature profile for Newtonian and Eyring–Powell fluid. It describes that the velocity is direct function of Pr and temperature profile is inverse function of Pr. Also, the comparison between Newtonian fluid and Eyring–Powell fluids for both velocity and temperature distributions are presented in Figs. 5 and 6. The comparison of Newtonian fluid and Eyring–Powell fluid shows that magnitude of velocity is greater in case of Eyring–Powell fluid. Flow of Eyring–Powell fluid enhanced the velocity and expresses its shear thinning behavior and suppresses the temperature field when compared with Newtonian fluid.

Figure 7 demonstrates the impact of Pr on temperature profile for (a) First level and (b) Second level of truncation. It is noticed that the temperature at the wall (at $\eta = 0$) is more when the system of equation solved by first level of truncation while it reduces when solved for second level of truncation. Also, Fig. 7 explains that temperature and thermal boundary layer thickness are decreased significantly for the larger values of Prandtl number. Lower temperature is noticed due to dominance of weaker thermal diffusivity over stronger momentum diffusivity. The same behaviour of Prandtl number is seen in Fig. 6.

Effect of convective boundary condition (i.e. Biot number γ) on temperature profile for Newtonian and Eyring–Powell fluid is shown in Fig. 8. Convective heating of the vertical plate is associated with Biot number γ. Enlarging the values of Biot number γ indicates higher internal thermal resistance of the vertical plate. As a result, an increase in the Biot number γ leads to increase of fluid temperature efficiently. Figure 8 validates this physical fact also. For both Newtonian and Eyring–Powell fluid, the temperature is enhanced with increase in Biot number γ. Further, it can also be seen that the temperature and thermal boundary layer thickness for Newtonian fluid is higher than the Eyring- Powell fluid which tells that the presence of Eyring–Powell fluid in the flow problem can effectively reduce the temperature.

Figures 9 and 10 deal with the variation of skin coefficient and local Nusselt number with respect to mixed convection parameter ξ for different Prandtl number. Friction at surface of the wall against the mixed convection parameter ξ reduces with increase in Prandtl number (Fig. 9). Nusselt number is rises which implies that the rate of heat transfer is enhanced with increase in Prandtl number (Fig. 10). The effect is more obvious with smaller Prandtl numbers because as the boundary layer becomes thicker (observed in Fig. 6), the heat transfer rate reduces. It is generally understood that fluids having lower Prandtl numbers possess high conductivity which results in large thermal boundary-layers. In this case heat diffuses rapidly from the heated plate compared to the case of fluids with high Prandtl numbers. Figures 11 and 12 represents the variation of skin friction factor and local Nusselt number with respect to mixed convection parameter ξ for different Eyring–Powell parameter. It is seen that increasing value of Eyring–Powell fluid parameter is responsible for decrease in skin friction coefficient (Fig. 11) as the velocity of the fluid decreases. While the rate of heat transfer increases (Fig. 12) due to fall in temperature by rising values of fluid parameter.

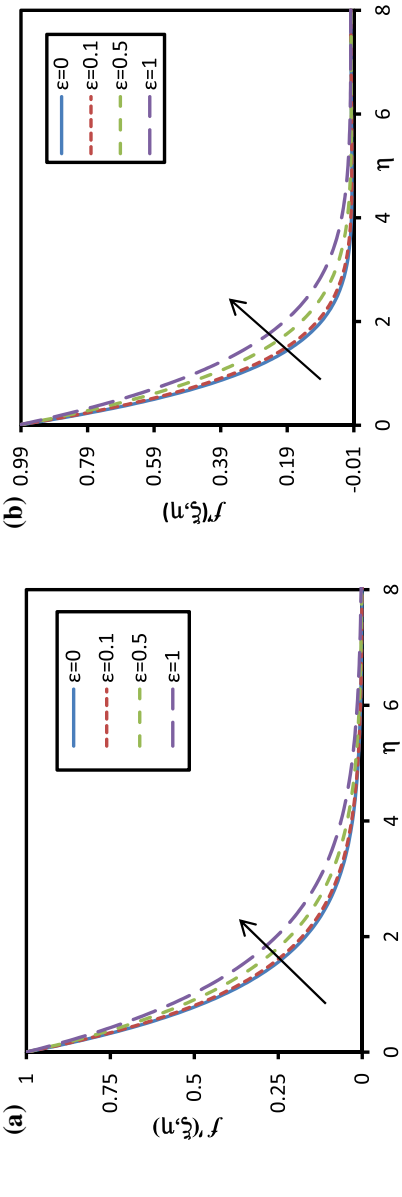

Fig. 3 Impact of fluid parameter ε on velocity profile for **a** first level and **b** second level of truncation

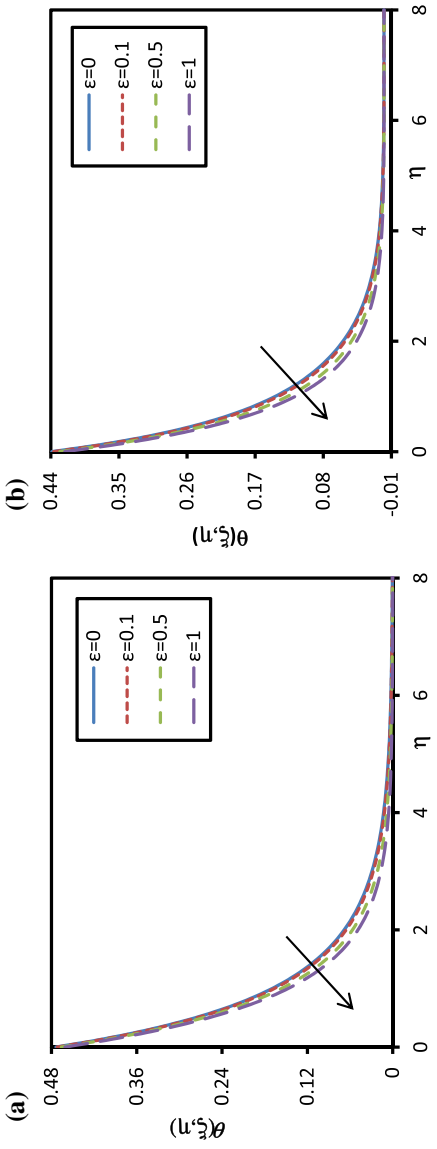

Fig. 4 Impact of ε on temperature profile for **a** first level and **b** second level of truncation

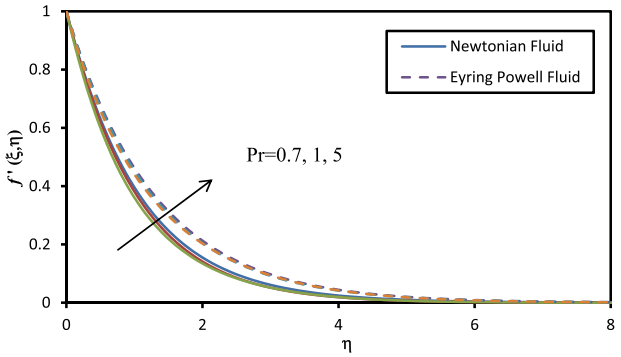

Fig. 5 Effect of Pr on velocity profile for Newtonian and Eyring–Powell fluid

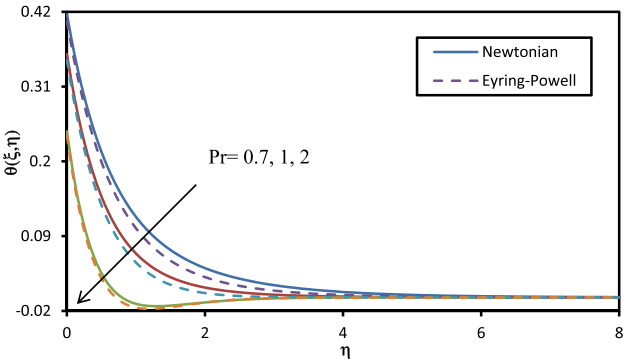

Fig. 6 Influence of Pr on temperature profile for Newtonian and Eyring–Powell Fluid

Conclusions

The mixed convection flow of Eyring–Powell fluid flow over a vertical stretching plate having variable velocity and temperature with effect of convective boundary condition has been discussed with the help of non-similarity method and solved by HAM. Validation of the result has also done with the previous published works. The conclusions obtained from the study are:

- Momentum boundary layer thickness is less in local non-similarity method as compare to local similarity method.
- The comparison of Newtonian fluid and Eyring–Powell fluid shows that magnitude of velocity is greater in case of Eyring–Powell fluid while it shows lesser magnitude of temperature than the Newtonian fluid.
- Skin friction coefficient is reduced with increase in values of Prandtl number and Local Nusselt number is increased with Prandtl number.
- Heat transfer coefficient increases while skin friction coefficient decreases with increase in fluid parameter.

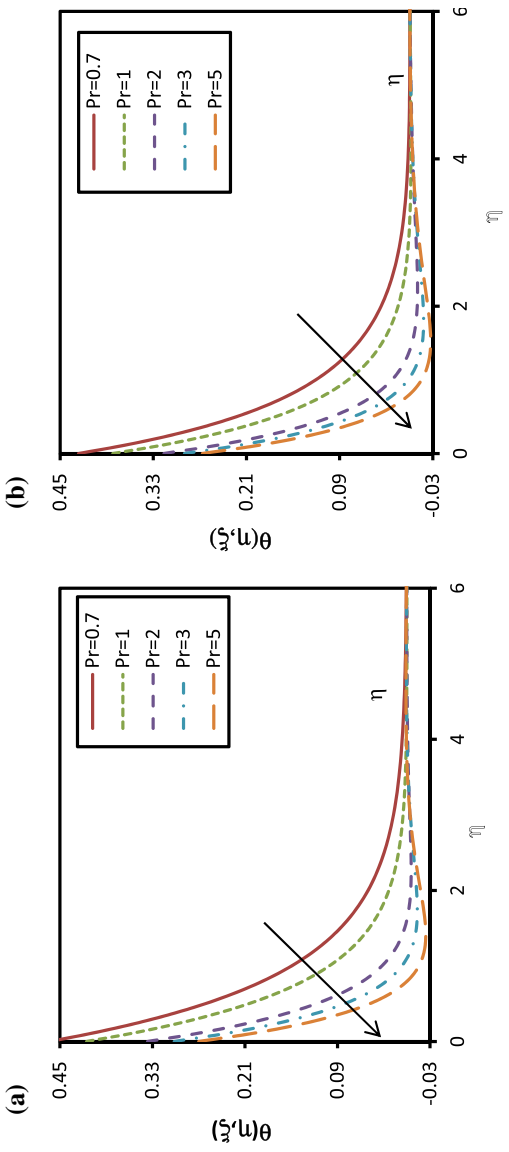

Fig. 7 Influence of Prandtl number Pr on temperature profile for **a** first level and **b** second level of truncation

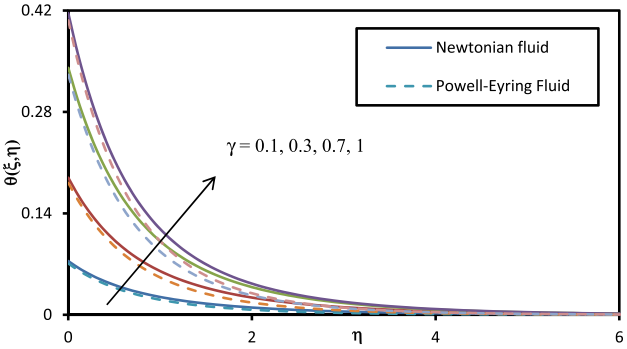

Fig. 8 Variation of temperature profile for Biot number γ

Fig. 9 Effect of Pr on skin coefficient friction against ξ

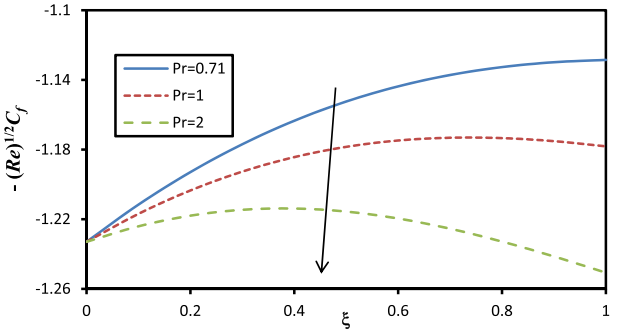

Fig. 10 Effect of Pr on Nusselt number against ξ

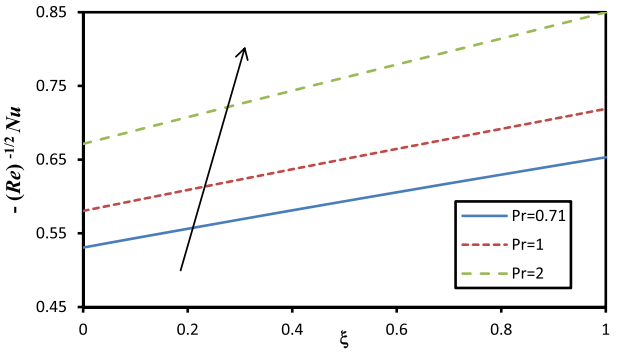

- With the rise in mixed convection parameter, the momentum and thermal boundary-layer thickness increase and decrease respectively.
- The behaviour of velocity and temperature profiles for different fluid parameter is same for both first and second level of truncation.

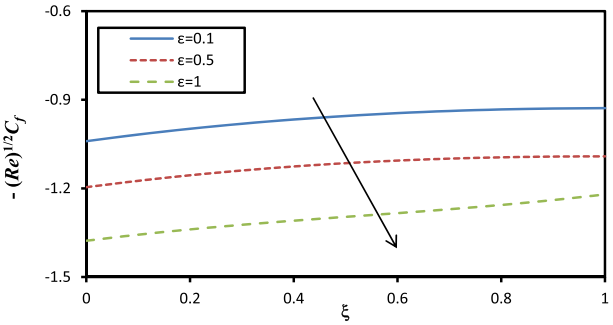

Fig. 11 Variation of Skin coefficient friction against ξ for different fluid parameter ϵ

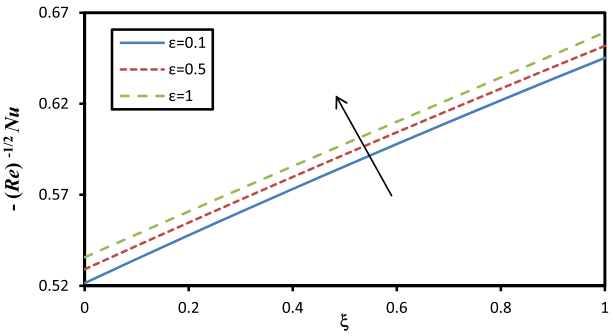

Fig. 12 Variation of Nusselt number against ξ for different fluid parameter ϵ

Acknowledgements The authors are thankful to all reviewers for their useful comments which have helped to improve the present article.

References

1. Pop, I., Ingham, D.B.: Convective Heat Transfer. Elsevier, Amsterdam (2001)
2. Sakiadis, B.C.: Boundary layer behaviour on continuous solid surfaces: I. Boundary-layer equations for two dimensional and axisymmetric flows. AIChEJ **7**(1), 26–28 (1961)
3. Erickson, L.E., Fan, L.T., Fox, V.G.: Heat andmass transfer on moving continuous flat plate with suction or injection. Ind. Eng. Chem. Fundam. **5**, 19–25 (1966)
4. Karwe, M.V., Jaluria, Y.: Fluid flow and mixed convection transport from a moving plate in rolling and extrusion processes. ASME J Heat Transf. **110**, 655–661 (1988)
5. Vajravelu, K., Roper, T.: Flow and heat transfer in a second grade fluid over a stretching sheet. Int. J. Non-Linear Mech. **34**(6), 1031–1036 (1999)
6. Magyari, E., Keller, B.: Exact solutions for self-similar boundary-layer flows induced by permeable stretching walls. Eur J. Mech B Fluids **19**(1), 109–122 (2000)
7. Patil, P.M., Roy, S., Pop, I.: Unsteady mixed convection flow over a vertical stretching sheet in a parallel free stream with variable wall temperature. Int. J. Heat Mass Transf. **53**, 4741–4748 (2010)
8. Mustafa, N., Asghar, S., Hossain, M.A.: Natural convection flow of second-grade fluid along a vertical heated surface with variable heat flux. Int. J. Heat Mass Transf. **53**(25), 5856–5862 (2010)
9. Ahmadi, A.R., Zahmatkesh, A., Hatami, M., Ganji, D.D.: A comprehensive analysis of the flow and heat transfer for a nanofluid over an unsteady stretching flat plate. Powder Technol. **258**, 125–133 (2014)
10. Rao, A.S., Prasad, V.R., Nagendra, N., Murthy, K.V.N., Reddy, N.B.: Numerical modeling of non-similar mixed convection heat transfer over a stretching surface with slip conditions. World J. Mech. **5**(6), 117–128 (2015)
11. Irgens, F.: Rheology and Non-Newtonian Fluids. Springer, Berlin (2014)

12. Gorla, R.S.R., Pratt, D.M.: Second law analysis of a non-Newtonian laminar falling liquid film along an inclined heated plate. Entropy **9**(1), 30–41 (2007)
13. Ghadikolaei, S.S., Hosseinzadeh, K., Yassari, M., Sadeghi, H., Ganji, D.D.: Analytical and numerical solution of non-Newtonian second-grade fluid flow on a stretching sheet. Therm. Sci. Eng. Progr. **5**, 309–316 (2018)
14. Powell, R.E., Eyring, H.: Mechanisms for the relaxation theory of viscosity. Nature **154**, 427–428 (1944)
15. Andersson, H.I., Aarseth, J.B., Braud, N., Dandapat, B.S.: Flow of a power-law fluid film on an unsteady stretching surface. J. Nonnewtonian Fluid Mech. **62**(1), 1–8 (1996)
16. Ray, A.K., Vasu, B.: Hydrodynamics of non-newtonian spriggs fluid flow past an impulsively moving plate. In: Singh, M., Kushvah, B., Seth, G., Prakash, J. (eds.) Applications of Fluid Dynamics. Lecture Notes in Mechanical Engineering, pp. 95–107. Springer, Singapore (2018)
17. Hayat, T., Iqbal, Z., Qasim, M., Obidat, S.: Steady flow of an Eyring–Powell fluid over a moving surface with convective boundary conditions. Int. J. Heat Mass Transf. **55**, 1817–1822 (2012)
18. Ghadikolaei, S.S., Hosseinzadeh, K., Ganji, D.D.: Analysis of unsteady MHD Eyring–Powell squeezing flow in stretching channel with considering thermal radiation and Joule heating effect using AGM. Case Stud. Therm. Eng. **10**, 579–594 (2017)
19. Gholinia, M., Hosseinzadeh, K., Mehrzadi, H., Ganji, D.D., Ranjbar, A.A.: Investigation of MHD Eyring–Powell fluid flow over a rotating disk under effect of homogeneous–heterogeneous reactions. Case Stud. Therm. Eng. **13**, 100356 (2019)
20. Aziz, A.: A similarity solution for laminar thermal boundary layer over a flat plate with a convective surface boundary condition. Commun. Nonlinear Sci. Numer. Simulat. **14**, 1064–1068 (2009)
21. Bataller, R.C.: Radiation effects for the Blasius and Sakiadis flows with convective surface boundary condition. Appl. Math. Comput. **206**(2), 832–840 (2008)
22. Khan, W.A., Gorla, R.S.R.: Heat and mass transfer in power-law nanofluids over a non-isothermal stretching wall with convective boundary condition. J. Heat Transf. **134**(11), 112001 (2012)
23. Murthy, P.V.S.N., RamReddy, C., Chamkha, A.J., Rashad, A.M.: Magnetic effect on thermally stratified nanofluid saturated non-Darcy porous medium under convective boundary condition. Int. Commun. Heat Mass Transf. **47**, 41–48 (2013)
24. RamReddy, C., Murthy, P.V.S.N., Chamkha, A.J., Rashad, A.M.: Soret effect on mixed convection flow in a nanofluid under convective boundary condition. Int. J. Heat Mass Transf. **64**, 384–392 (2013)
25. Kameswaran, P.K., Sibanda, P., Murti, A.S.N.: Nanofluid flow over a permeable surface with convective boundary conditions and radiative heat transfer. Math. Prob., Eng (2013)
26. Vasu, B., Ram Reddy, C., Murthy, P.V.S.N., Gorla, R.S.R.: Entropy generation analysis in nonlinear convection flow of thermally stratified fluid in saturated porous medium with convective boundary condition. J. Heat Transf. **139**(9), 091701 (2017)
27. Chen, T.S., Sparrow, E.M.: Flow and heat transfer over a flat plate with uniformly distributed, vectored surface mass transfer. ASME J. Heat Transf. **98**, 674–676 (1976)
28. Sparrow, E.M., Yu, H.S.: Local non-similarity thermal boundary layer solutions. Trans. ASME J. Heat Transf. **93**, 328–334 (1971)
29. Mushtaq, M., Asghar, S., Hossain, M.A.: Mixed convection flow of second grade fluid along a vertical stretching flat surface with variable surface temperature. Heat Mass Transf. **43**(10), 1049 (2007)
30. Vasu, B., Ray, A.K.: Numerical study of Carreau nanofluid flow past vertical plate with the Cattaneo–Christov heat flux model. Int. J. Numer. Methods Heat Fluid Flow **29**(2), 702–723 (2018)
31. Liao, S.: Homotopy analysis method in nonlinear differential equations, pp. 153–165. Higher Education Press, Beijing (2012)
32. Turkyilmazoglu, M.: A note on the homotopy analysis method. Appl. Math. Lett. **23**, 1226–1230 (2010)
33. Liao, S.J., Pop, I.: Explicit analytic solution for similarity boundary layer equations. Int. J. Heat Mass Transf. **47**, 75–85 (2004)
34. Liao, S.J.: Series solution of nonlinear eigenvalue problems by means of the homotopy analysis method. Nonlinear Anal. Real World Appl. **10**, 2455–2470 (2009)
35. Gorla, R.S.R., Kumari, M.: Non-similar solutions for mixed convection in non-Newtonian fluids along a vertical plate in a porous medium. Transport Porous Med. **33**, 295–307 (1998)
36. Cheng, W.T., Lin, H.T.: Non-similarity solution and correlation of transient heat transfer in laminar boundary layer flow over a wedge. Int. J. Eng. Sci. **40**(5), 531–548 (2002)
37. Farooq, U., Hayat, T., Alsaedi, A., Liao, S.J.: Series solutions of non-similarity boundary layer flows of nano-fluids over stretching surfaces. Numer. Algorithms **70**(1), 43–59 (2015)

38. Chamkha, A., Gorla, R.S.R., Ghodeswar, K.: Non-similar solution for natural convective boundary layer flow over a sphere embedded in a porous medium saturated with a nanofluid. Transport Porous Med. **86**(1), 13–22 (2011)
39. Kameswaran, P.K., Vasu, B., Murthy, P.V.S.N., Gorla, R.S.R.: Mixed convection from a wavy surface embedded in a thermally stratified nanofluid saturated porous medium with non-linear Boussinesq approximation. Int. Commun. Heat Mass Transf. **77**, 78–86 (2016)
40. Minkowycz, W.J., Sparrow, E.M., Schneider, G.E., Pletcher, R.H.: Handbook of Numerical Heat Transfer. Wiley-Interscience, New York (1988)
41. Wanous, K.J., Sparrow, E.M.: Heat transfer for flow longitudinal to a cylinder with surface. J. Heat Transf. **87**(2), 317–319 (1965)
42. Catherall, D., Stewartson, K., Williams, P.G.: Viscous flow past a flat plate with uniform injection. Proc. R. Soc. Lond. A **284**(1398), 370–396 (1965)
43. Lee, S.Y., Ames, W.F.: Similarity solutions for non-Newtonian fluids. AIChEJ. **12**(4), 700–708 (1966)
44. Sparrow, E.M., Quack, H.: Local non-similarity boundary-layer solutions. AIAA J. **8**(11), 1936–1942 (1970)
45. Massoudi, M.: Local non-similarity solutions for the flow of a non-Newtonian fluid over a wedge. Int. J. Non-Linear Mech. **36**, 961–976 (2001)
46. Mureithi, E.W., Mason, D.P.: Local non-similarity solutions for a forced-free boundary layer flow with viscous dissipation. Math. Comput. Appl. **15**(4), 558–573 (2010)
47. Ganji, D.D., Afrouzi, G.A., Talarposhti, R.A.: Application of variational iteration method and homotopy–perturbation method for nonlinear heat diffusion and heat transfer equations. Phys. Lett. A **368**(6), 450–457 (2007)
48. Liao, S.: Notes on the homotopy analysis method: some definitions and theorems. Commun. Nonlinear Sci. Numer. Simul. **14**(4), 983–997 (2009)
49. Allan, F.M., Syam, M.I.: On the analytic solution of non-homogeneous Blasius problem. J. Comput. Appl. Math. **182**(2), 362–371 (2005)
50. Cheng, J., Liao, S., Mohapatra, R.N., Vajravelu, K.: Series solutions of nano boundary layer flows by means of the homotopy analysis method. J. Math. Anal. Appl. **343**(1), 233–245 (2008)
51. Ziabakhsh, Z., Domairry, G.: Solution of the laminar viscous flow in a semi-porous channel in the presence of a uniform magnetic field by using the homotopy analysis method. Commun. Nonlinear Sci. Numer. Simul. **14**(4), 1284–1294 (2009)
52. Kousar, N., Liao, S.J.: Series solution of non-similarity boundary-layer flows over a porous wedge. Transp. Porous Media **83**(2), 397–412 (2010)
53. Hassan, H., Rashidi, M.M.: An analytic solution of micropolar flow in a porous channel with mass injection using homotopy analysis method. Int. J. Numer. Methods H **24**(2), 419–437 (2014)
54. Dinarvand, S., Abbassi, A., Hosseini, R., Pop, I.: Homotopy analysis method for mixed convective boundary layer flow of a nanofluid over a vertical circular cylinder. Therm. Sci. **19**(2), 549–561 (2015)
55. Vasu, B., Ray, A.K., Gorla, R.S.R.: Homotopy simulation of non-Newtonian Spriggs fluid flow over a flat plate with oscillating motion. Int. J. Appl. Mech. Eng. **24**(2), 359–385 (2019)
56. Ray, A.K., Vasu, B., Bég, O.A., Gorla, R.S.R., Murthy, P.V.S.N.: Magneto-bioconvection flow of a Casson thin film with nanoparticles over an unsteady stretching sheet. Int J. Numer. Method H **29**(11), 4277–4309 (2019)
57. Hayat, T., Iqbal, Z., Qasim, M., Alsaedi, A.: Flow of an Eyring–Powell fluid with convective boundary conditions. J. Mech. **29**, 217–224 (2013)
58. Nataraja, H.R., Sarma, M.S., Rao, B.N.: Flow of a second-order fluid over a stretching surface having power-law temperature. Acta Mech. **128**(3–4), 259–262 (1998)